Vlnovody s velkým kontrastem indexu lomu

„Fotonický drát“

(vlnovod s velkým kontrastem indexu lomu)

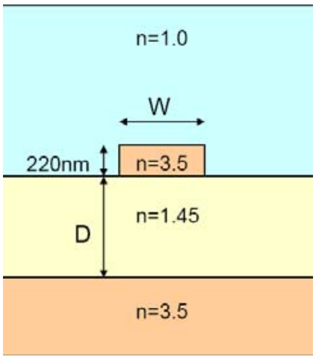

Rozložení elektromagnetického pole základního vidu TE_{00}

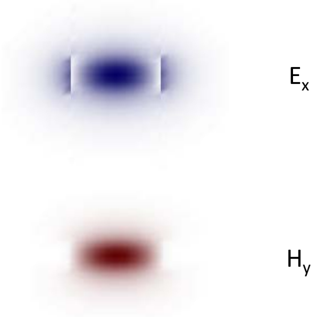

Vazba do „nanofotonických“ vlnovodů

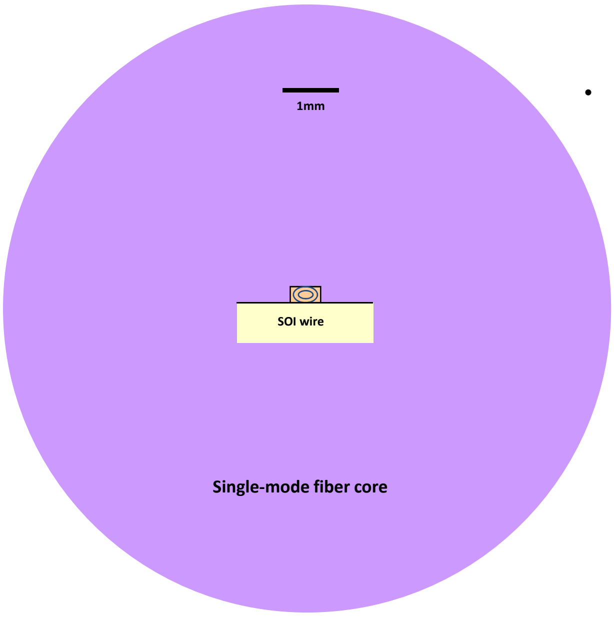

- **Problémy:**
  - Účinná vazba mezi submikrometrovým vlnovodem a vláknem
  - Je nutný konvertor velikosti vidového pole:
    - v horizontální rovině
    - ve vertikální rovině (obtížnější)
  - Polarizační problém

„Adiabatický přechod“ mezi vlnovody velmi různých profilů / kontrastů

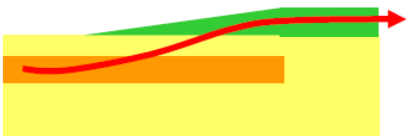

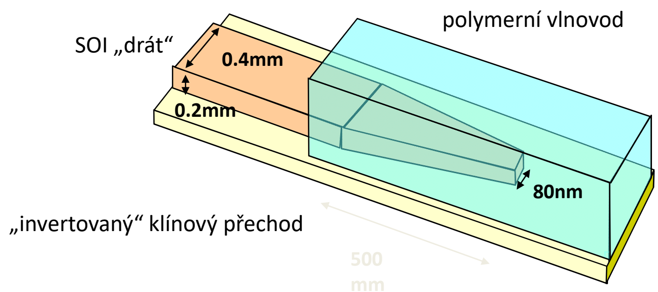

Křemíkové vlnovody se subvlnovými strukturami (subwavelength grating waveguide, SWG)

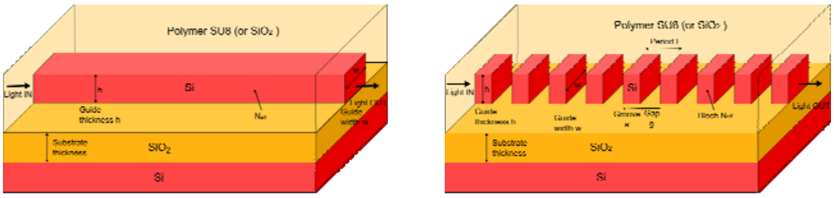

Schematic picture of (a) a strip channel waveguide and (b) SWG waveguide considered in this contribution. In both cases, Si guide (either continuous or segmented) on SiO_2 substrate, embedded in SU8 polymer (or, alternatively in SiO_2 cladding) are considered; h represents the guide thickness, w guide width, L is the SWG period (with Si groove dimension a, and gap g).

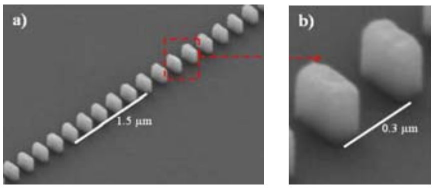

Scanning electron microscope (SEM) images of fabricated structures including: a) SWG straight waveguide with Λ = 300 nm, w = 250 nm and a duty cycle of 33%. b) Detail of two SWG segments.

P. J. Bock, Optics Express, 18(19), 20251 (2010).

- SWG waveguide - a new type of microphotonic waveguide
- Practical implementations to fiber-chip coupling, waveguide crossing and refractive index engineering

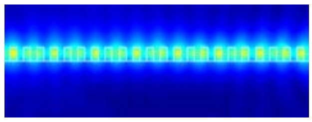

ELEMENTÁRNÍ TEORIE EFEKTIVNÍHO PROSTŘEDÍ (Effective medium theory, EMT)

Vrstevnaté prostředí s parametry $\varepsilon_1,\ d_1$ a $\varepsilon_2,\ d_2$, $d_1,\ d_2 \ll \lambda$

Střední hodnota elektrické indukce pro elektrické pole rovnoběžné s vrstvami :

$$E_{x1} = E_{x2} = E,\quad \bar{D}_x = \frac{D_{x1}d_1 + D_{x2}d_2}{d_1 + d_2} = \frac{\varepsilon_1 d_1 + \varepsilon_2 d_2}{d_1 + d_2}E = \varepsilon_\parallel E \qquad f = \frac{d_1}{d_2}$$

$$\frac{d_1}{d_1 + d_2} = f,\quad \frac{d_2}{d_1 + d_2} = 1 - f,\quad 0 \le f \le 1.$$

Tedy $\varepsilon_\parallel = f\varepsilon_1 + (1 - f)\varepsilon_2,$

Střední hodnota intenzity elektrického pole pro elektrickou indukci kolmou k vrstvám :

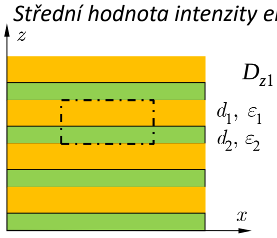

$$D_{z1} = D_{z2} = D,\quad \bar{E}_z = \frac{D_{z1}d_1 + D_{z2}d_2}{d_1 + d_2} = \frac{d_1/\varepsilon_1 + d_2/\varepsilon_2}{d_1 + d_2}D_z = \frac{1}{\varepsilon_\perp}D_z,$$

Tedy $\dfrac{1}{\varepsilon_\perp} = \dfrac{1}{\varepsilon_1}f + \dfrac{1}{\varepsilon_2}(1 - f),\quad \varepsilon_\perp = \dfrac{\varepsilon_1\varepsilon_2}{f\varepsilon_2 + (1 - f)\varepsilon_1},$

Efektivní prostředí je anizotropní, jednoosé, **s tenzorem permitivity**

$$\boldsymbol{\varepsilon}_{eff} = \begin{pmatrix} \varepsilon_\parallel & 0 & 0 \\ 0 & \varepsilon_\parallel & 0 \\ 0 & 0 & \varepsilon_\perp \end{pmatrix}$$

J. C. Maxwell Garnett, "Colours in metal glasses and in metallic films,"
Philosophical Transaction of the Royal Society London **203**, 385-420 (1904).

6

Složitější subvlnové vlnovodné struktury

Vazební člen - vidový transformátor

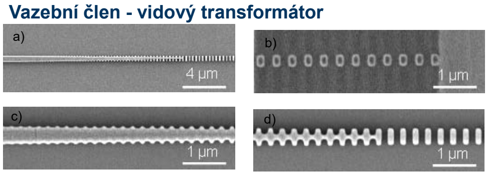

Subwavelength grating mode transformer.
a) SEM image of the coupler,
b) low - confinement section near the chip edge,
c) high-confinement section near the strip waveguide,
d) Intermediate section.

P. J. Bock et al., 7th IEEE Conference on Group IV Photonics, Sept. 2010, Beijing

Křížení segmentovaných vlnovodů

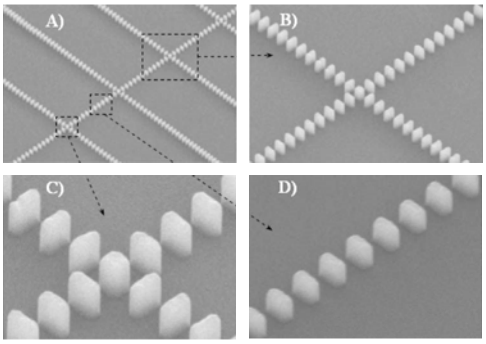

Scanning electron microscope images of SWG crossings:
A) multiple SWG crossings,
B) one SWG crossing,
C) detail of the crossing region with square center segment,
D) SWG straight waveguide.

P. J. Bock et al., Optics Express, 18(15), 16146 (2010).

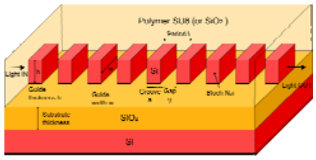

Disperzní vlastnosti SWG vlnovodů

Standard SWGW, w = 350 nm, Λ = 400 nm, g = 200 nm, TE polarization

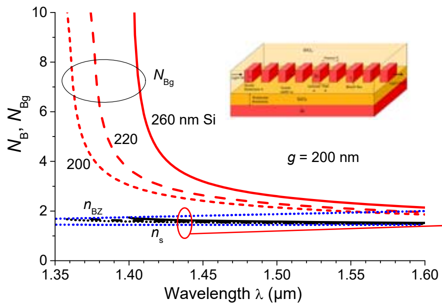

phase and group effective indices N_B , N_{Bg}

bandgap region

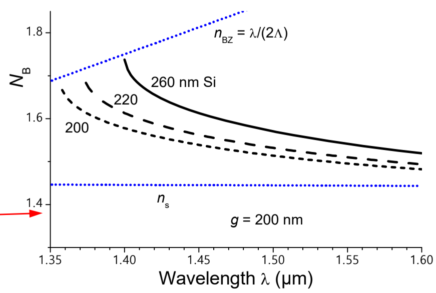

phase effective index N_B

BLOCH MODE FIELD PROPAGATION

Vertical component of the magnetic field intensity @ λ = 1500 nm

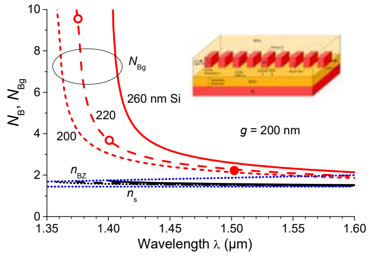

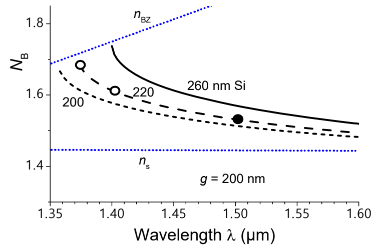

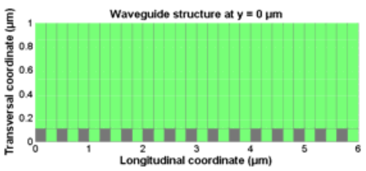

character quite similar
to a uniform waveguide

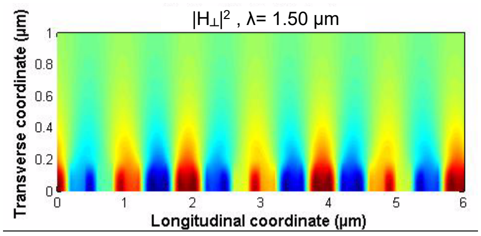

BLOCH MODE FIELD PROPAGATION

Vertical component of the magnetic field intensity @ λ = 1400 nm

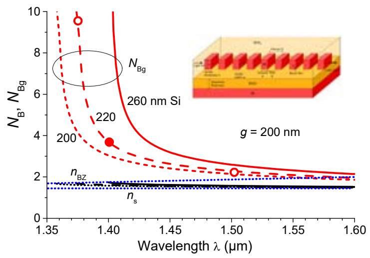

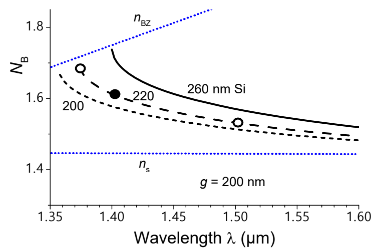

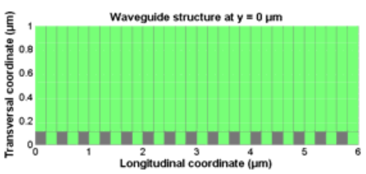

backward propagating waves
are becoming important

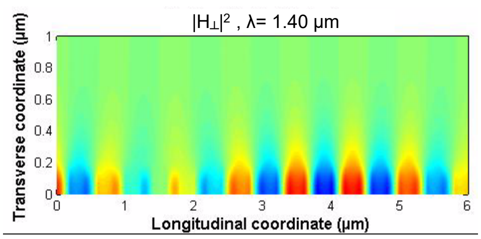

BLOCH MODE FIELD PROPAGATION

Vertical component of the magnetic field intensity @ λ = 1375 nm

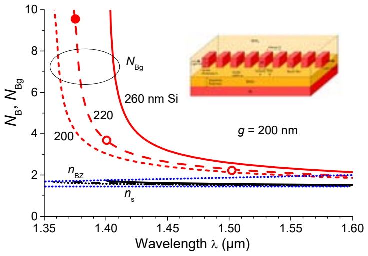

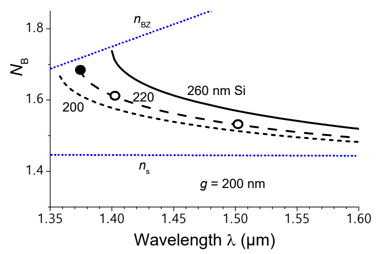

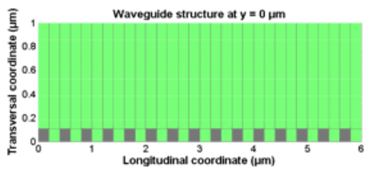

markedly resonant character

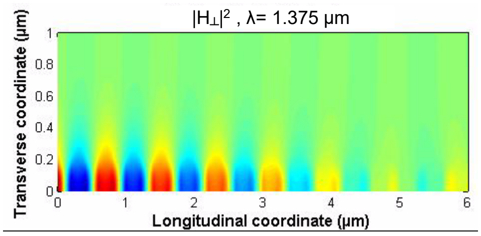

BLOCH MODE FIELD PROPAGATION

Vertical component of the magnetic field intensity @ λ = 1350 nm

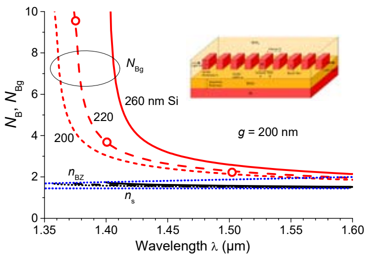

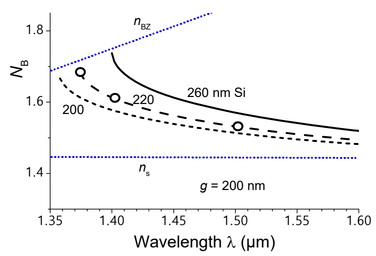

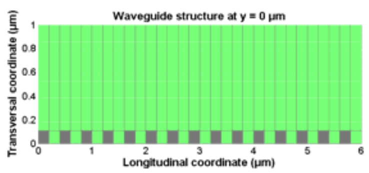

evanescent Bloch mode
within the bandgap

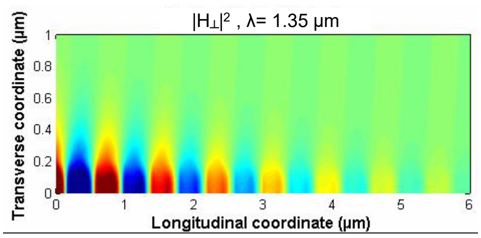

VAZBA MEZI SWG VLNOVODEM A NANODRÁTEM

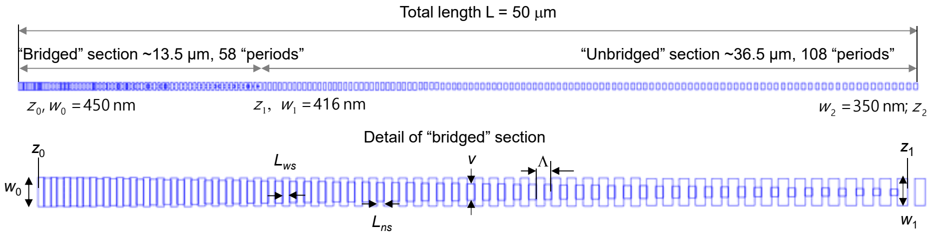

Both wide and narrow "bridged" segments are linearly tapered;
the period length Λ is also linearly tapered,
from 200 nm to 270 nm in the "bridged" section and
from 270 nm to 400 nm in the "unbridged" section

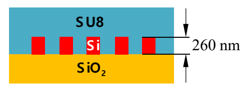

Version 2 (L/2)

Similar (linearly tapered) but twice shorter: total length ~ 25 μm
"Bridged" section ~ 6.75 μm, 29 "periods", "unbridged" section ~ 18.25 μm, 54 "periods"

Version 3 (L/4)

Similar (linearly tapered) but four-times shorter: total length ~ 12.5 μm
"Bridged" section ~ 3.38 μm, 15 "periods", "unbridged" section ~ 9.13 μm, 27 "periods"

Version 4 (L/8)

Similar (linearly tapered) but eight-times shorter: total length ~ 6.25 μm
"Bridged" section ~ 1.69 μm, 7 "periods", "unbridged" section ~ 4.6 μm, 13 "periods"

TRANSMITTANCE AND REFLECTANCE OF THE NANOWIRE TO SWGW COUPLER

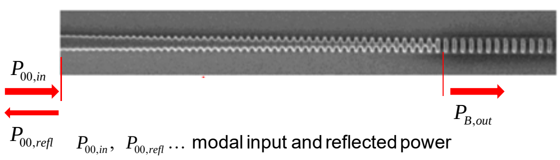

$$T = \frac{P_{B,out}}{P_{00,in}}, \quad R = \frac{P_{00,refl}}{P_{00,in}}$$

$P_{00,in}$, $P_{00,refl}$ … modal input and reflected power

$P_{B,out}$ … power of the fundamental forward Bloch mode

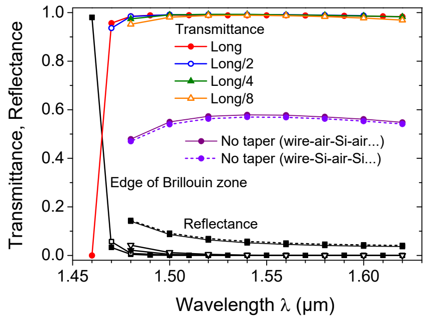

TE polarization

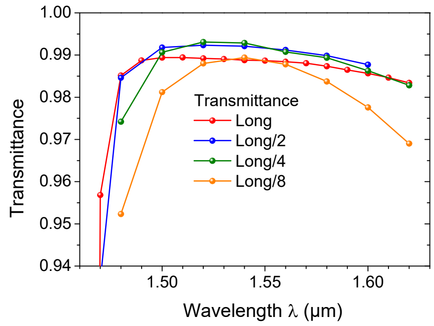

TE_{00} MODE FIELD DISTRIBUTION IN THE L/4 COUPLER: VERTICAL PLANE

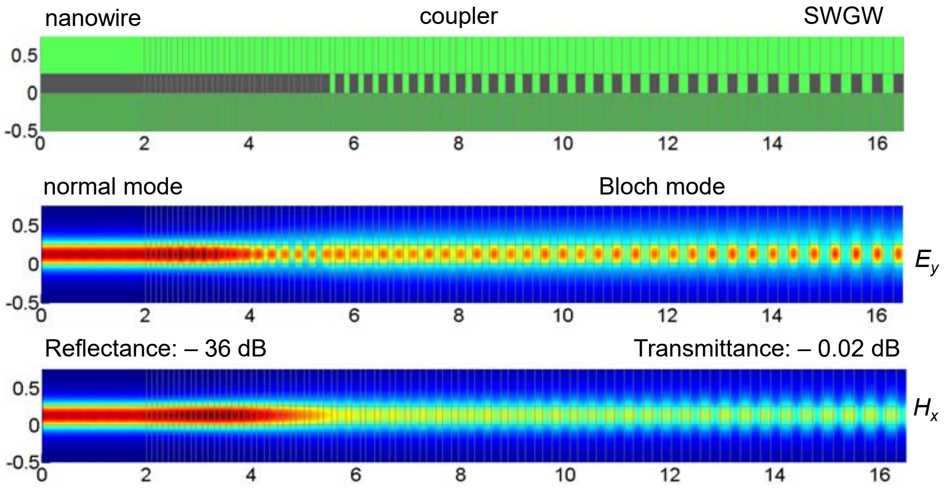

TE_{00} MODE FIELD DISTRIBUTION IN THE L/4 COUPLER: HORIZONTAL PLANE (upper half)

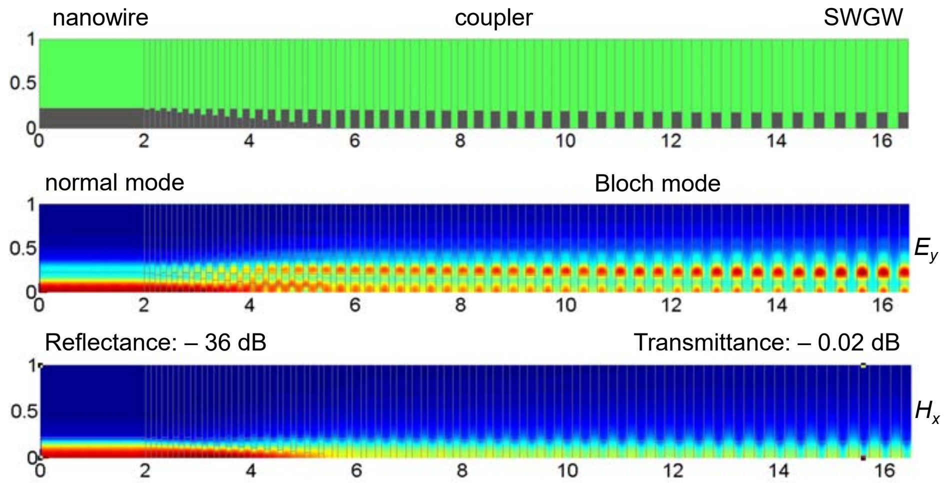

INFLUENCE OF RANDOM FLUCTUATIONS ON SWGW PERFORMANCE

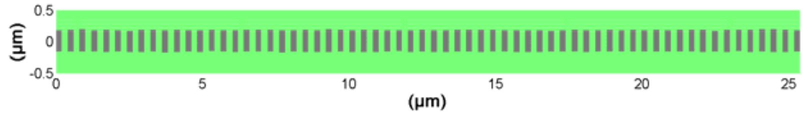

Positions and dimensions of Si segments fluctuate with normal distribution and standard deviation σ

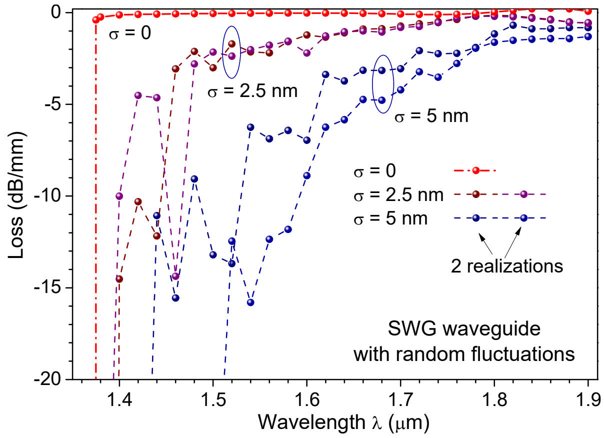

Aplikace subvlnových segmentovaných vlnovodů na směrovou odbočnici

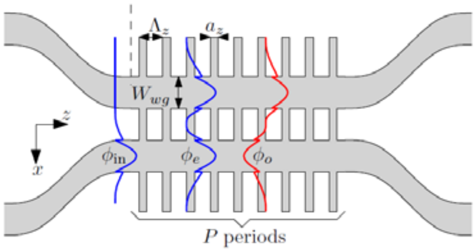

„Vložný útlum“ v obou větvích

Optimalizace parametrů umožňuje využít větší šířku pásma:

„Vazební délka“

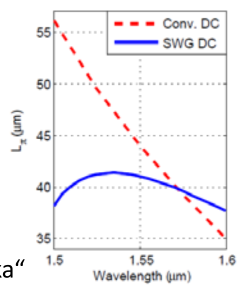

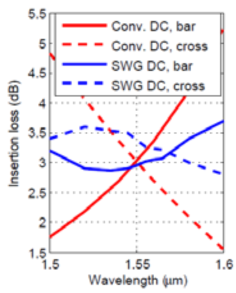

Aplikace subvlnových segmentovaných vlnovodů na vazební člen s mnohovidovou interferencí

P. Cheben et al., Wavelength-Independent Multimode Interference Coupler, Opt. Express 2012
NRC, Ottawa, Canada, and University of Malaga, Spain

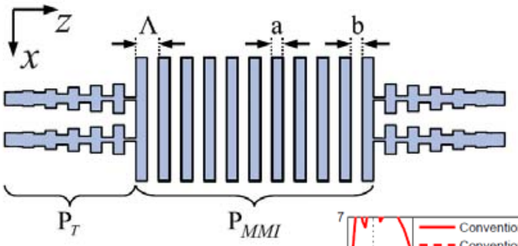

Optimalizace parametrů umožňuje širokopásmové použití

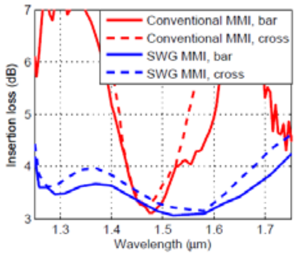

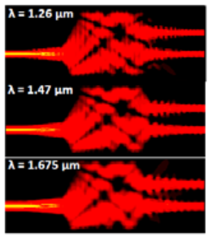

BROADBAND SWGW MMI COUPLER

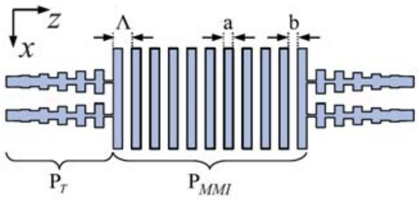

1. Optimization of MMI section for broadband operation
2. Check of imaging properties of the MMI section
3. Verification of taper function
4. Analysis of possible mutual coupling between tapers
5. Field distribution and scattering matrix
   of the complete coupler

A. Maese-Novo, R. Halir, S. Romero-García, D. Pérez-Galacho, L. Zavargo-Peche, A. Ortega-Moñux,
I. Molina-Fernández, J. G.Wangüemert-Pérez, and P. Cheben, *Opt. Express* vol 21, 7033-7040 (2013)

BLOCH MODES IN THE SWG MULTIMODE REGION

$|E_y(x,y)|,\ \lambda = 1.55\ \mu\text{m}$

$\Lambda = 180$ nm

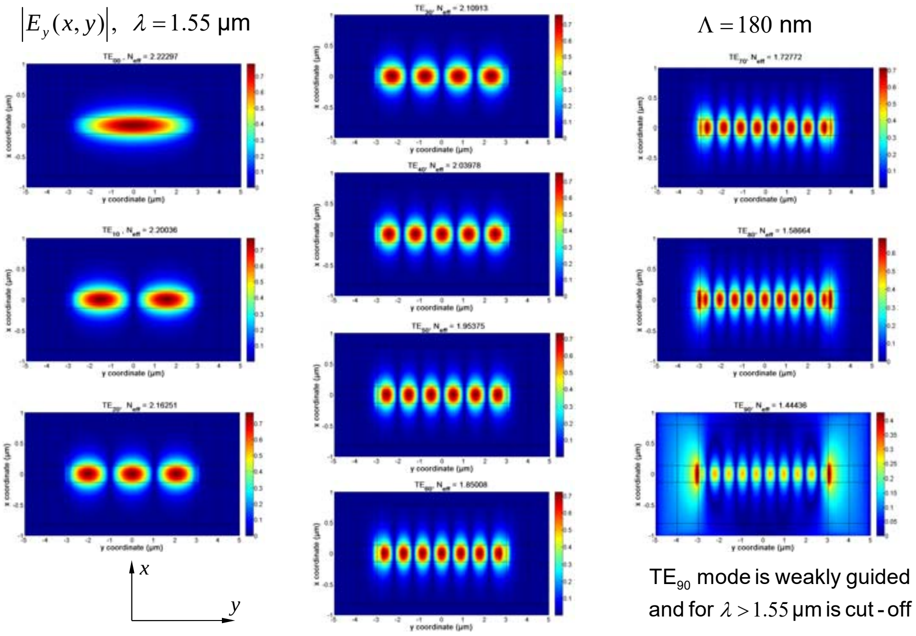

TE$_{90}$ mode is weakly guided and for $\lambda > 1.55$ μm is cut-off

OPTIMIZATION OF MMI SECTION FOR BROADBAND OPERATION

Minimize wavelength dependence of the beat length between several lowest-order lateral Bloch modes by optimization of period length; MMI section width = 6 μm

$$\text{"ideal" beat length: } L_{\pi m} = \frac{\left[(m+1)^2 - 1\right]\pi}{3(\beta_0 - \beta_m)} = \frac{m(m+2)}{6(N_{00} - N_{0m})},\quad m = 1,\ 2,\ \ldots,\ 8$$

Eff. indices

Beat lengths

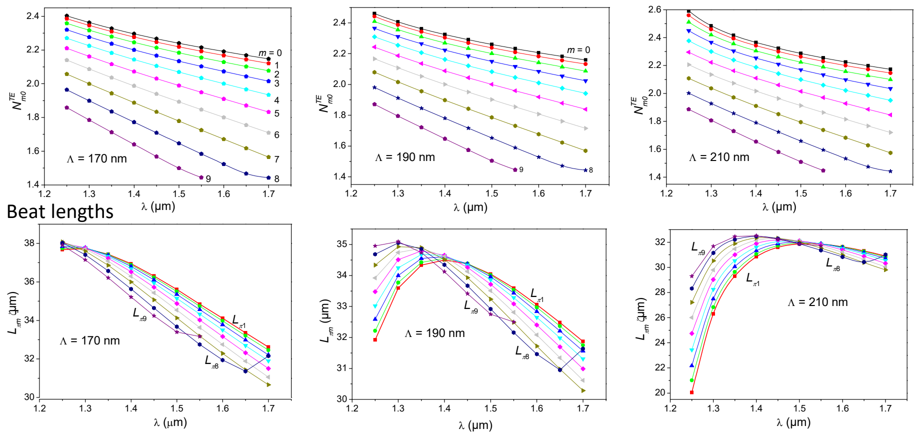

OPTIMIZATION OF THE MMI SECTION FOR 1.3 – 1.7 µm WAVELENGTH RANGE

Average beat lengths

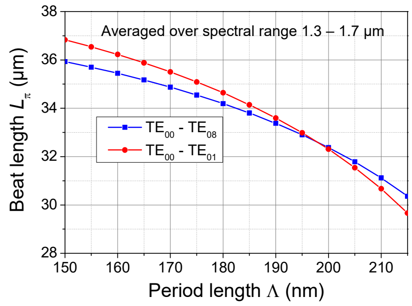

Standard deviations of the beat lengths

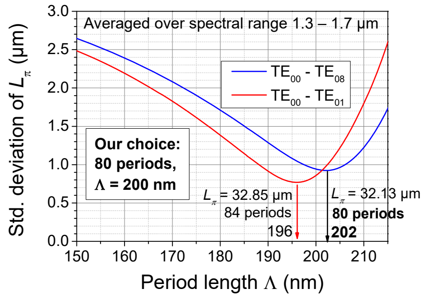

Averaging over wavelengths and modes:

$$\Lambda_{opt}^{0-1} = 196 \text{ nm}, \quad L_\pi^{0-1} = 32.85 \text{ µm}, \quad NoP^{0-1} \doteq L_\pi^{0-1} \big/ (2\Lambda_{opt}^{0-1}) = 84 \text{ periods},$$

$$\Lambda_{opt}^{0-8} = 202 \text{ nm}, \quad L_\pi^{0-8} = 32.13 \text{ µm}, \quad NoP^{0-8} \doteq L_\pi^{0-8} \big/ (2\Lambda_{opt}^{0-8}) = 80 \text{ periods}.$$

IMAGING PROPERTIES OF THE SWG MMI SECTION

Excitation of the SWG MMI section with SWG “ports”
by the superposition of symmetric and antisymmetric Bloch modes

MMI: 80 periods, Λ = 200 nm

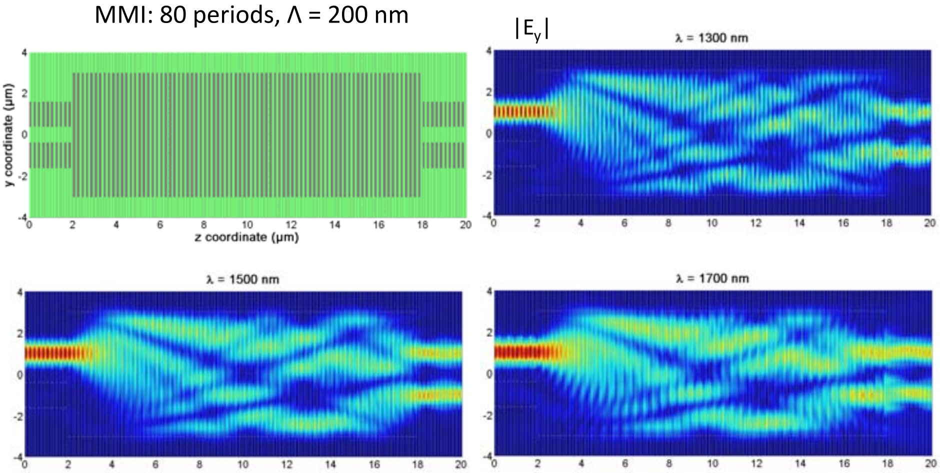

PROPERTIES OF INPUT AND OUTPUT COUPLERS

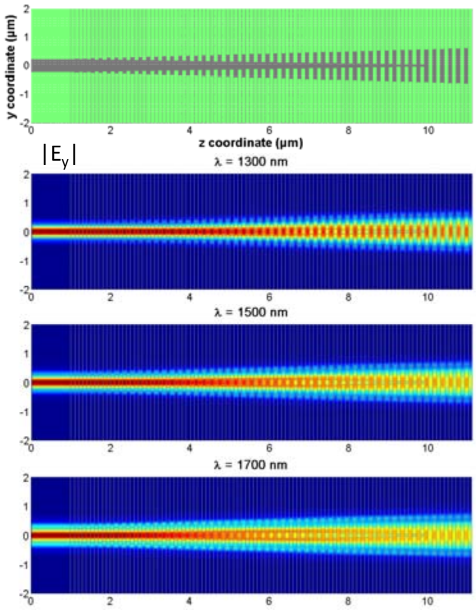

Estimated SWG period Λ = 200 nm

Conversion from photonic wire into Bloch mode of the SWG output:

Very high conversion efficiency difficult to reliably calculate (loss <= 0.01 dB), very small return loss – reflected power <= – 45 dB for all wavelengths 1.3 µm, 1.5 µm, and 1.7 µm.

Shorter taper could probably work well, too.

CHECK OF MUTUAL COUPLING IN THE TAPERS

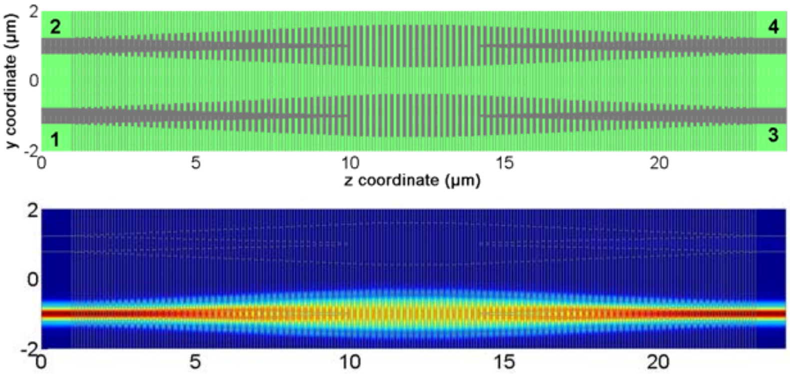

Calculated scattering parameters:

λ (µm)	$\lvert S_{11}\rvert^2$	$\lvert S_{31}\rvert^2$	$\lvert S_{41}\rvert^2$	Loss
1.70	2.304×10^{-5}	0.995	4.963×10^{-3}	-1.561×10^{-5}
1.50	2.804×10^{-5}	0.993	6.991×10^{-3}	-2.611×10^{-4}
1.30	4.149×10^{-5}	0.988	1.260×10^{-2}	-3.966×10^{-4}

Mutual coupling in tapers is unimportant

FIELD DISTRIBUTION IN THE SWG MMI COUPLER

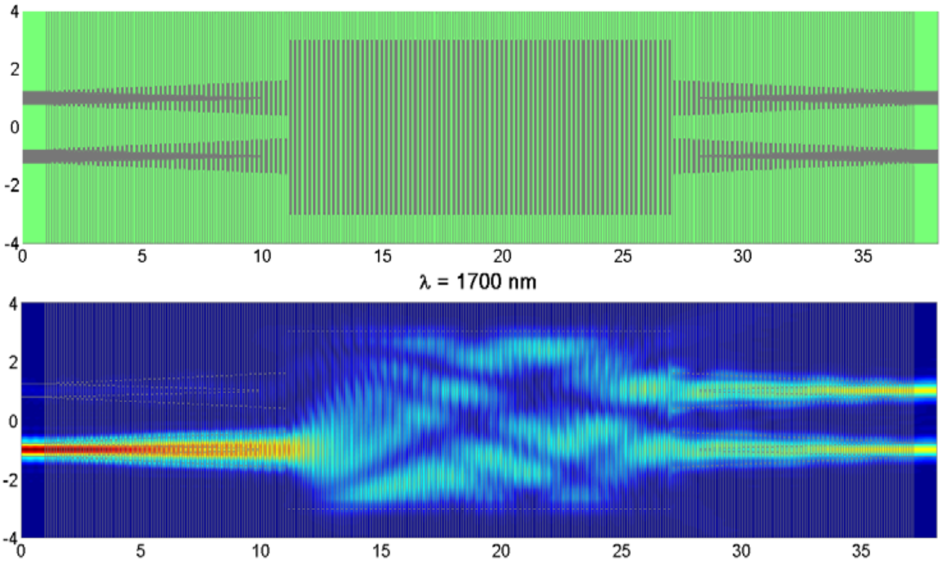

S-PARAMETERS OF THE COMPLETE MMI DEVICE

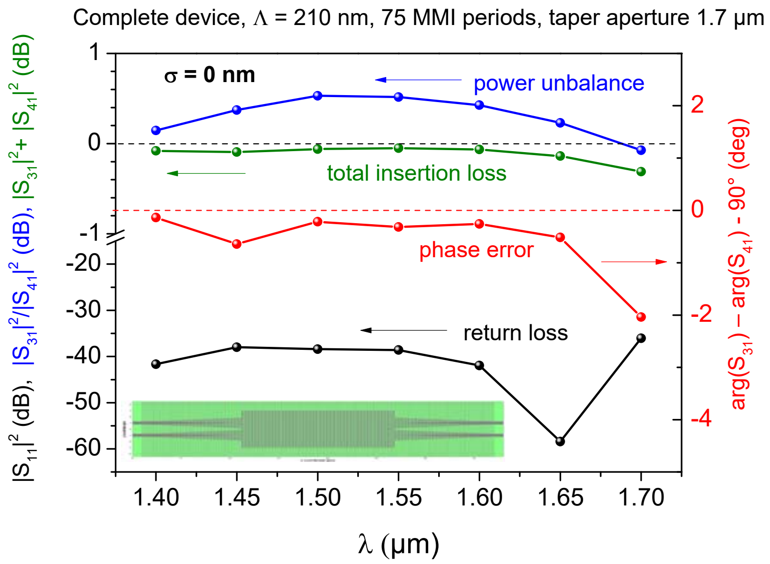

INFLUENCE OF RANDOM FLUCTUATIONS

Complete device, Λ = 210 nm, 75 MMI periods, taper aperture 1.7 μm

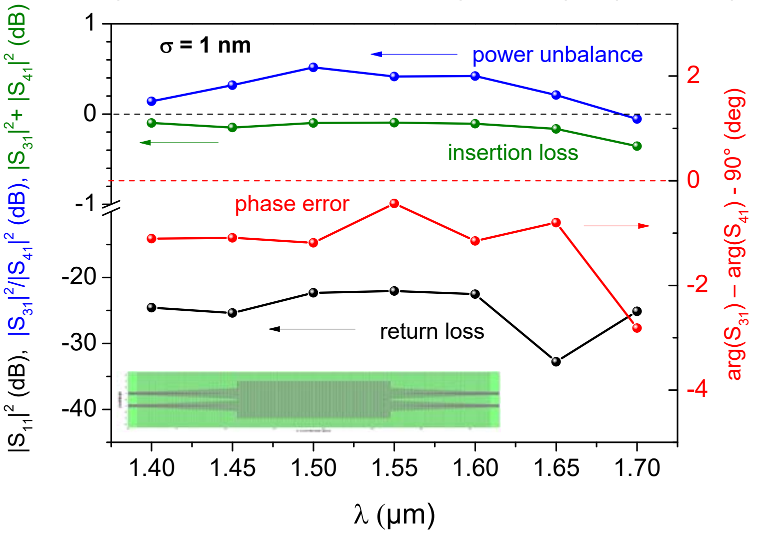

INFLUENCE OF RANDOM FLUCTUATIONS

Complete device, Λ = 210 nm, 75 MMI periods, taper aperture 1.7 μm

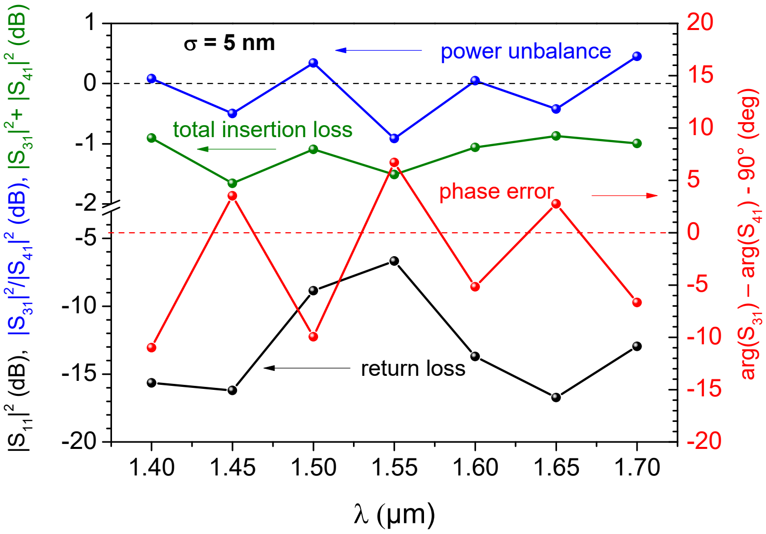

SWG BASED BRAGG FILTERS

- J. Wang, I. Glesk, and L.R. Chen: *Subwavelength grating filtering devices*. Opt. Express **22**, 15335-15345 (2014)

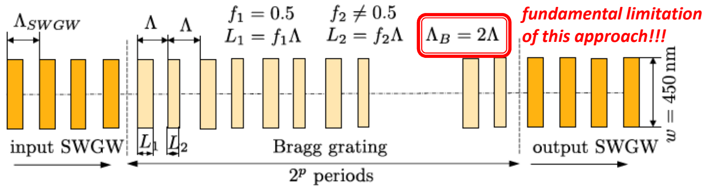

- For numerical simulations, a commercial 2.5-D FDTD software packet was used

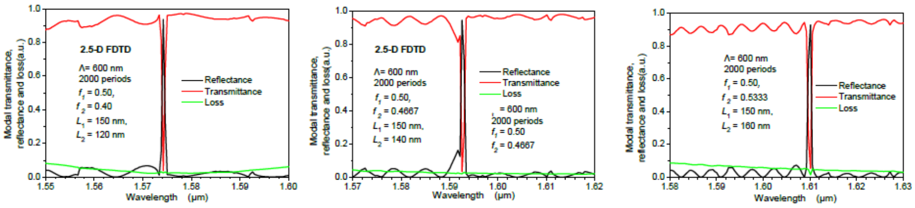

NUMERICKÉ SIMULACE

„2.5D“ komerční FDTD software

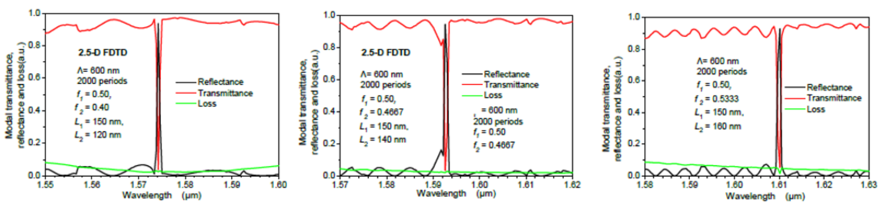

3D Fourierovská modální metoda (FJFI, ÚFE)